

## An optimization strategy on prion AGAAAAGA amyloid fibril molecular modeling

Jiapu Zhang<sup>1\*</sup>, Changzhi Wu<sup>2</sup>

<sup>1</sup>School of Sciences, Information Technology and Engineering,  
University of Ballarat, Mount Helen, VIC 3350, Australia

<sup>2</sup>School of Mathematics and Computer Science,  
Chongqing Normal University, Chongqing 630047, China

\*Corresponding author. Tel.: +61 423487360, +61 3 5327 9809,  
E-mail addresses: j.zhang@ballarat.edu.au, jiapu.zhang@hotmail.com

**Abstract:** X-ray crystallography and nuclear magnetic resonance (NMR) spectroscopy are two powerful tools to determine the protein 3D structure. However, not all proteins can be successfully crystallized, particularly for membrane proteins. Although NMR spectroscopy is indeed very powerful in determining the 3D structures of membrane proteins, same as X-ray crystallography, it is still very time-consuming and expensive. Under many circumstances, due to the noncrystalline and insoluble nature of some proteins, X-ray and NMR cannot be used at all. Computational approaches, however, allow us to obtain a description of the protein 3D structure at a submicroscopic level.

To the best of the author's knowledge, there is little structural data available to date on the AGAAAAGA palindrome in the hydrophobic region (113–120) of prion proteins, which falls just within the N-terminal unstructured region (1–123) of prion proteins. Many experimental studies have shown that the AGAAAAGA region has amyloid fibril forming properties and plays an important role in prion diseases. However, due to the noncrystalline and insoluble nature of the amyloid fibril, little structural data on the AGAAAAGA is available. This paper introduces a simple optimization strategy approach to address the 3D atomic-resolution structure of prion AGAAAAGA amyloid fibrils. Atomic-resolution structures of prion AGAAAAGA amyloid fibrils got in this paper are useful for the drive to find treatments for prion diseases in the field of medicinal chemistry.

**Keywords** Simulated annealing evolutionary computation, prion AGAAAAGA palin-

drome, amyloid fibril.

## 1 Introduction

Prion diseases are invariably fatal and highly infectious neurodegenerative diseases affecting humans and animals. The neurodegenerative diseases such as Creutzfeldt-Jakob disease (CJD), variant Creutzfeldt-Jakob diseases (vCJD), Gerstmann-Straussler-Scheinker syndrome (GSS), Fatal Familial Insomnia (FFI), Kuru in humans, scrapie in sheep, bovine spongiform encephalopathy (BSE or mad-cow disease) and chronic wasting disease (CWD) in cattle belong to prion diseases. By now there have not been some effective therapeutic approaches or medications to treat all these prion diseases.

Prion diseases are amyloid fibril diseases. The normal cellular prion protein ( $\text{PrP}^C$ ) is rich in  $\alpha$ -helices but the infectious prions ( $\text{PrP}^{Sc}$ ) are rich in  $\beta$ -sheets amyloid fibrils. The conversion of  $\text{PrP}^C$  to  $\text{PrP}^{Sc}$  is believed to involve a conformational change from a predominantly  $\alpha$ -helical protein (42%  $\alpha$ -helix, 3%  $\beta$ -sheet) to a protein rich in  $\beta$ -sheets (30%  $\alpha$ -helix, 43%  $\beta$ -sheet) [11].

Many experimental studies such as [4, 5, 6, 12, 13, 14, 15, 16, 20] have shown two points: (1) the hydrophobic region (113-120) AGAAAAGA of prion proteins is critical in the conversion from a soluble  $\text{PrP}^C$  into an insoluble  $\text{PrP}^{Sc}$  fibrillar form; and (2) normal AGAAAAGA is an inhibitor of prion diseases. Furthermore, we computationally clarified that prion AGAAAAGA segment indeed has an amyloid fibril forming property [22, 23, 24]. However, laboratory experiences have shown that using traditional experimental methods is very difficult to obtain atomic-resolution structures of AGAAAAGA due to the noncrystalline and insoluble nature of the amyloid fibril [18, 25]. By introducing novel mathematical canonical dual formulations and computational approaches, in this paper we may construct atomic-resolution molecular structures for prion (113-120) AGAAAAGA amyloid fibrils.

Many studies have indicated that computational approaches or introducing novel mathematical formulations and physical concepts into molecular biology can significantly stimulate the development of biological and medical science. Various computer computational approaches were used to address the problems related to “amyloid fibril” [7, 8, 9, 10, 19, 21]. Here, we would like to use the simulated annealing evolutionary

computations to build the optimal atomic-resolution amyloid fibril models in hopes to be used for controlling prion diseases.

The atomic structures of all amyloid fibrils revealed steric zippers, with strong van der Waals (vdw) interactions between  $\beta$ -sheets and hydrogen bonds (HBs) to maintain the  $\beta$ -strands [17]. The vdw contacts of atoms are described by the Lennard-Jones (LJ) potential energy:

$$V_{LJ}(r) = 4\varepsilon \left[ \left(\frac{\sigma}{r}\right)^{12} - \left(\frac{\sigma}{r}\right)^6 \right], \quad (1)$$

where  $\varepsilon$  is the depth of the potential well and  $\sigma$  is the atom diameter; these parameters can be fitted to reproduce experimental data or deduced from results of accurate quantum chemistry calculations. The  $(\frac{\sigma}{r})^{12}$  term describes repulsion and the  $(\frac{\sigma}{r})^6$  term describes attraction. If we introduce the coordinates of the atoms whose number is denoted by  $N$  and let  $\varepsilon = \sigma = 1$  be the reduced units, the form (1) becomes

$$f(x) = 4 \sum_{i=1}^N \sum_{j=1, j < i}^N \left( \frac{1}{\tau_{ij}^6} - \frac{1}{\tau_{ij}^3} \right), \quad (2)$$

where  $\tau_{ij} = (x_{3i-2} - x_{3j-2})^2 + (x_{3i-1} - x_{3j-1})^2 + (x_{3i} - x_{3j})^2$ ,  $(x_{3i-2}, x_{3i-1}, x_{3i})$  is the coordinates of atom  $i$ ,  $N \geq 2$ . The minimization of LJ potential  $f(x)$  on  $\mathbb{R}^n$  (where  $n = 3N$ ) is an optimization problem:

$$\min f(x) \quad \text{subject to } x \in \mathbb{R}^{3N}. \quad (3)$$

Similarly as (1), i.e. the potential energy for the vdw interactions between  $\beta$ -sheets:

$$V_{LJ}(r) = \frac{A}{r^{12}} - \frac{B}{r^6}, \quad (4)$$

the potential energy for the HBs between the  $\beta$ -strands has the formula

$$V_{HB}(r) = \frac{C}{r^{12}} - \frac{D}{r^{10}}, \quad (5)$$

where  $A, B, C, D$  are given constants. Thus, the amyloid fibril molecular modeling problem is deduced into well solve the optimization problem (3).

This paper is organized as follows. In Section 2, we first describe how to build the prion AGAAAAGA amyloid fibril molecular models, and then the simulated annealing evolutionary computational algorithm for optimizing the models is given. At the end of Section 2 the models are done a little refinement by Amber 11 [3]. At last, we

conclude that when using the time-consuming and costly X-ray crystallography or NMR spectroscopy we still cannot determine the protein 3D structure, we may introduce computational approaches or novel mathematical formulations and physical concepts into molecular biology to study molecular structures. This concluding remark will be made in the last section.

## 2 Prion AGAAAAGA amyloid fibril models' Molecular Modeling and Optimizing

Constructions of the AGAAAAGA amyloid fibril molecular structures of prion 113–120 region are based on the most recently released experimental molecular structures of human M129 prion peptide 127–132 (PDB entry 3NHC released into Protein Data Bank (<http://www.rcsb.org>) on 04-AUG-2010). The atomic-resolution structure of this peptide is a steric zipper, with strong vdw interactions between  $\beta$ -sheets and HBs to maintain the  $\beta$ -strands (Figure 1).

In Figure 1 we see that G (H) chains (i.e.  $\beta$ -sheet 2) of 3NHC.pdb can be obtained from A (B) chains (i.e.  $\beta$ -sheet 1) by

$$G(H) = \begin{pmatrix} 1 & 0 & 0 \\ 0 & -1 & 0 \\ 0 & 0 & -1 \end{pmatrix} A(B) + \begin{pmatrix} 9.07500 \\ 4.77650 \\ 0.00000 \end{pmatrix}, \quad (6)$$

and other chains can be got by

$$I(J) = I_3 G(H) + \begin{pmatrix} 0 \\ 9.5530 \\ 0 \end{pmatrix}, K(L) = I_3 G(H) + \begin{pmatrix} 0 \\ -9.5530 \\ 0 \end{pmatrix}, \quad (7)$$

$$C(D) = I_3 A(B) + \begin{pmatrix} 0 \\ 9.5530 \\ 0 \end{pmatrix}, E(F) = I_3 A(B) + \begin{pmatrix} 0 \\ -9.5530 \\ 0 \end{pmatrix}, \quad (8)$$

where  $I_3$  is the 3-by-3 identity matrix. Basing on the template 3NHC.pdb from the Protein Data Bank, three prion AGAAAAGA palindrome amyloid fibril models - an AAAAGA model (Model 1), a GAAAAG model (Model 2), and an AAAAGA model (Model 3) - will be successfully constructed in this paper. AB chains of Models 1-3

were respectively got from AB chains of 3NHC.pdb using the mutate module of the free package Swiss-PdbViewer (SPDBV Version 4.01) (<http://spdbv.vital-it.ch>). It is pleasant to see that almost all the hydrogen bonds are still kept after the mutations; thus we just need to consider the vdw contacts only. Making mutations for GH chains of 3NHC.pdb, we can get the GH chains of Models 1-3. However, the vdw contacts between A chain and G chain, between B chain and H chain are too far at this moment (Figure 2).

Seeing Figure 2, we may know that for Models 1-3 at least two vdw interactions between A.ALA3.CB-G.ALA4.CB, B.ALA4.CB-H.ALA3.CB should be maintained. Fixing the coordinates of A.ALA3.CB and B.ALA4.CB, letting the coordinates of G.ALA4.CB and H.ALA3.CB be variables, we may get a simple LJ potential energy minimization problem (3) just with six variables. For solving this six variable optimization problem, the following simulated annealing evolutionary computational algorithm is presented.

### 3 The hybrid evolutionary computational algorithms

Discrete gradient (DG) method is a local search optimization method [2]. Simulated annealing is a global search method and demonstrates more advantages compared with local search method. This paper simply replaces the DG method in [1] by the SA method (e.g. [24]). Large scale of global optimization benchmark testing problems will be used to test the new algorithms and numerical computational results show the effective of the new algorithms presented in this section.

**Algorithm 1** *SA-SAES*( $\mu + \lambda$ ).

*Step 0.* Randomly generate  $\mu$  parents, where each parent  $z_k = (\vec{x}_k, \vec{\sigma}_k)$ .

*Step 1.* Apply SA on each parent  $\vec{x}_k$ .

*Step 2.* Set  $\tau = \left( \sqrt{\left( 2\sqrt{(n)} \right)} \right)^{-1}$  and  $\tau' = \left( \sqrt{(2n)} \right)^{-1}$ .

*Step 3.* Until  $\lambda$  children are generated, do

*Step 4.* Select two parents  $z_k = (\vec{x}_k, \vec{\sigma}_k)$  and  $z_l = (\vec{x}_l, \vec{\sigma}_l)$  at random to generate child  $\vec{y}_j = (\vec{x}_j, \vec{\sigma}_j)$ .

*Step 5.* Discrete recombination: for each variable  $x_{ji}$  and step size  $\sigma_{ji}$  in  $\vec{y}_j$ , do ( $x_{ji} = x_{ki}$  and  $\sigma_{ji} = \sigma_{ki}$ ) or ( $x_{ji} = x_{li}$  and  $\sigma_{ji} = \sigma_{li}$ )

*Step 6.* Mutation: For each  $x_{ji}$  and step size  $\sigma_{ji}$  in  $\vec{y}_j$

$$x'_{ji} = x_{ji} + \sigma_{ji}N_j(0, 1)$$

$$\sigma'_{ji} = \sigma_{ji} \exp(\tau'N(0, 1) + \tau N_j(0, 1))$$

*Step 7.* If the number of children is less than  $\lambda$ , go to Step 4.

*Step 8.* Select the best  $\mu$  individuals among all the  $\mu + \lambda$  parents and children.

*Step 9.* Apply SA on the best individual among the selected  $\mu$  individuals.

*Step 10.* If the stopping criteria are satisfied, stop, else go to step 2.

**Algorithm 2** SA-SACEP.

*Step 0.* Randomly generate  $\mu$  parents and evaluate them, where each parent  $z_k = (\vec{x}_k, \vec{\sigma}_k)$ .

*Step 1.* Apply SA on each parent  $\vec{x}_k$ .

*Step 2.* Set  $\tau = \left( \sqrt{\left( 2\sqrt{(n)} \right)} \right)^{-1}$  and  $\tau' = \left( \sqrt{(2n)} \right)^{-1}$ .

*Step 3.* For each parent, generate a child as follows

$$x'_{ji} = x_{ji} + \sigma_{ji}N_j(0, 1)$$

$$\sigma'_{ji} = \sigma_{ji} \exp(\tau'N(0, 1) + \tau N_j(0, 1))$$

*Step 4.* Evaluate all children

*Step 5.* Undertake a tournament  $y$  for each parent and child as follows: select  $\zeta$  individuals with replacement from the joint set of parents and children. For each individual  $z$  of the  $\zeta$  individuals, if  $y$  is better than  $z$ , add 1 to the fitness of  $y$ .

*Step 6.* Select the best  $\mu$  individuals among all parents and children with the highest fitness.

*Step 7.* Apply SA on the best individual among the selected  $\mu$  individuals.

*Step 8.* If the stopping criteria are satisfied, stop, else go to step 1.

Numerical results (in Table 1 and Table 2) show that the above two algorithms can find global minimums. However, SAES( $\mu + \lambda$ ) and SACEP algorithms just can get local minimal solutions. Thus, SA-SAES( $\mu + \lambda$ ) and SA-SACEP algorithms greatly improve the SAES( $\mu + \lambda$ ) and SACEP algorithms. This shows the effectiveness of SA and the hybrid technique.

Setting the coordinates of G.ALA4.CB and H.ALA3.CB as initial solutions, running the above two hybrid algorithms, for Models 1-3 we get

$$G(H) = \begin{pmatrix} 1 & 0 & 0 \\ 0 & -1 & 0 \\ 0 & 0 & -1 \end{pmatrix} A(B) + \begin{pmatrix} -0.703968 \\ 7.43502 \\ -0.33248 \end{pmatrix}. \quad (9)$$

By (4) we can get close vdw contacts between A chain and G chain, between B chain and H chain (Figure 3).

Furthermore, we may employ the Amber 11 package (Case et al. 2010) to optimize Models 1-3 and at last get Models 1-3 with stable total potential energies (Figure 4). The other CDIJ and EFKL chains can be got by parallelizing ABGH chains in the use of mathematical formulas (2)-(3).

## 4 Conclusion

If a parallel computing algorithm hybridizes with a sequential computing algorithm, then the new hybrid algorithm performs much better than they work alone separately. In this paper, the parallel computing algorithms used are the SAES( $\mu + \lambda$ ) and SA-CEP algorithms and the sequential computing algorithm used is the SA algorithm. We successfully tested the new hybrid algorithms by extensive more than 40 benchmark global optimization problems. The hybrid evolutionary computational algorithms were successfully applied to construct three prion AGAAAAGA amyloid fibril models.

**Acknowledgments:** This research was supported by a Victorian Life Sciences Computation Initiative (VLSCI) grant number VR0063 on its Peak Computing Facility at the University of Melbourne, an initiative of the Victorian Government.

## References

- [1] Abbass H.A., Bagirov A.M., Zhang J.P. (2003) The discrete gradient evolutionary strategy method for global optimization. The IEEE Congress on Evolutionary Computation (IEEE-CEC), IEEE-Press, Vol. 1, pages 435–442, Australia, 2003.
- [2] Bagirov A.M., Karasozen B., Sezer M. (2008) Discrete gradient method: a derivative free method for nonsmooth optimization. J. Opt. Theor. Appl. 137: 317-34.
- [3] Case D.A., T.A. Darden, T.E. Cheatham, III, C.L. Simmerling, J. Wang, R.E. Duke, R. Luo, R.C. Walker, W. Zhang, K.M. Merz, B.P. Roberts, B. Wang, S. Hayik, A. Roitberg, G. Seabra, I. Kolossvry, K.F. Wong, F. Paesani, J. Vanicek, J. Liu, X. Wu, S.R. Brozell, T. Steinbrecher, H. Gohlke, Q. Cai, X. Ye, J. Wang, M.-J. Hsieh, G. Cui, D.R. Roe, D.H. Mathews, M.G. Seetin, C. Sagui, V. Babin,

- T. Luchko, S. Gusarov, A. Kovalenko and P.A. Kollman. 2010. AMBER 11, University of California, San Francisco.
- [4] Brown D.R. (2000) Prion protein peptides: optimal toxicity and peptide blockade of toxicity. *Mol. Cell. Neurosci.* 15: 66-78.
- [5] Brown D.R. (2001) Microglia and prion disease. *Microsc. Res. Tech.* 54: 71-80.
- [6] Brown D.R., Herms J., Kretzschmar H.A. (1994) Mouse cortical cells lacking cellular PrP survive in culture with a neurotoxic PrP fragment. *Neuroreport* 5: 2057-2060.
- [7] Carter D.B., Chou K.C. (1998) A model for structure dependent binding of Congo Red to Alzheimer beta-amyloid fibrils. *Neurobiol. Aging* 19: 37-40.
- [8] Chou K.C. (2004) Insights from modelling the tertiary structure of BACE2. *J. Proteome Res.* 3: 1069-72.
- [9] Chou K.C. (2004) Review: structural bioinformatics and its impact to biomedical science. *Curr. Med. Chem.* 11: 2105-34.
- [10] Chou K.C., Howe W.J. (2002) Prediction of the tertiary structure of the beta-secretase zymogen. *Biochem. Biophys. Res. Commun.* 292: 702-8.
- [11] Griffith J.S. (1967) Self-replication and scrapie. *Nature* 215: 1043-4.
- [12] Holscher C., Delius H., Burkle A. (1998) Overexpression of nonconvertible PrP<sup>C</sup> delta114-121 in scrapie-infected mouse neuroblastoma cells leads to trans-dominant inhibition of wild-type PrP<sup>Sc</sup> accumulation, *J. Virol.* 72: 1153-9.
- [13] Jobling M.F., Huang X., Stewart L.R., Barnham K.J., Curtain C., Volitakis I., Perugini M., White A.R., Cherny R.A., Masters C.L., Barrow C.J., Collins S.J., Bush A.I., Cappai R. (2001) Copper and zinc binding modulates the aggregation and neurotoxic properties of the prion peptide PrP 106-126, *Biochem.* 40: 8073-84.
- [14] Jobling M.F., Stewart L.R., White A.R., McLean C., Friedhuber A., Maher F., Beyreuther K., Masters C.L., Barrow C.J., Collins S.J., Cappai R. (1999) The hydrophobic core sequence modulates the neurotoxic and secondary structure properties of the prion peptide 106-126, *J. Neurochem.* 73: 1557-65.



- [15] Kuwata K., Matumoto T., Cheng H., Nagayama K., James T.L., Roder H. (2003) NMR-detected hydrogen exchange and molecular dynamics simulations provide structural insight into fibril formation of prion protein fragment 106–126, *Proc. Natl. Acad. Sci. USA* 100, 14790–5.
- [16] Norstrom E.M., Mastrianni J.A. (2005) The AGAAAAGA palindrome in PrP is required to generate a productive PrP<sup>Sc</sup>–PrP<sup>C</sup> complex that leads to prion propagation, *J. Biol. Chem.* 280: 27236–43.
- [17] Sawaya M.R., Sambashivan S., Nelson R., Ivanova M.I., Sievers S.A., Apostol M.I., Thompson M.J., Balbirnie M., Wiltzius J.J., McFarlane H.T., Madsen A., Riek C., Eisenberg D. (2007) Atomic structures of amyloid cross-beta spines reveal varied steric zippers, *Nature* 447: 453–7.
- [18] Tsai H.H.G. (2005) Understanding the biophysical mechanisms of protein folding, misfolding, and aggregation at molecular level (in Chinese), *Chem. (The Chinese Chem. Soc. of Taipei)* 63: 601-12.
- [19] Wang J.F., Wei D.Q., Li L., Chou K.C. (2008) Review: Drug candidates from traditional Chinese medicines, *Curr. Top. Med. Chem.* 8: 1656–65.
- [20] Wegner C., Romer A., Schmalzbauer R., Lorenz H., Windl O., Kretzschmar H.A. (2002) Mutant prion protein acquires resistance to protease in mouse neuroblastoma cells, *J. Gen. Virol.* 83: 1237–45.
- [21] Wei D.Q., Sirois S., Du Q.S., Arias H.R., Chou K.C. (2005) Theoretical studies of Alzheimer’s disease drug candidate [(2,4-dimethoxy) benzylidene]-anabaseine dihydrochloride (GTS-21) and its derivatives, *Biochem. Biophys. Res. Commun.* 338: 1059–64.
- [22] Zhang J.P. (2009) Studies on the structural stability of rabbit prion probed by molecular dynamics simulations, *J. Biomol. Struct. Dyn.* 27: 159-62.
- [23] Zhang J.P. (2011) Optimal molecular structures of prion AGAAAAGA amyloid fibrils formatted by simulated annealing, *J. Mol. Model.* 17: 173-9 (*Crystallography Time*, Volume 3, No. 1, January 2011, page 2).
- [24] Zhang J.P., Sun J., Wu C.Z. (2011) Optimal atomic-resolution structures of prion AGAAAAGA amyloid fibrils, *J. Theor. Biol.* 279: 17-28 (*Nuclear Energy Research Today*, Volume 7, Issue 4, April 2011).

[25] Zheng J., Ma B.Y., Tsai C.J., Nussinov R. (2006) Structural stability and dynamics of an amyloid-forming peptide GNNQQNY from the yeast prion Sup-35, Biophys. J. 91: 824-33.

Table 1: The Optimal objective function values of SAES( $\mu + \lambda$ ) Algorithm and SA-SAES( $\mu + \lambda$ ) Algorithm, and SACEP Algorithm and SA-SACEP Algorithm

Function	# of variables	SAES( $\mu + \lambda$ )	SA-SAES( $\mu + \lambda$ )	SACEP	SA-SACEP
F1 (Neumaier 2004)	2	-186.731	-186.731	-186.731	-186.731
F2 (Neumaier 2004)	5	1.0	1.0	1.0	1.0
	10	1.0	1.0	1.0	1.0
	20	1.28551	1.0	24.5297	1.0
	30	1.02754	1.0	1.13336	1.0
	50	1.00388	1.00001	9.28671	1.00001
F3 (Ackleys)	2	0.0	0.0	0.0	0.0
	3	0.0	0.0	0.0	0.0
	5	0.0	2.41563e-05	0.0	2.41563e-05
	7	2.13384	4.86888e-05	1.72382	4.86888e-05
	10	3.90647	7.6222e-05	1.08046	8.82517e-05
	20	5.1886	0.000190629	2.24666	0.000224306
	30	5.47366	0.0003507	4.92406	0.000406911
F4 (Bohachevsky Nr.1)	2	0.11754	0.117535	0.117548	0.117535
F5 (Bohachevsky Nr.2)	2	0.0	0.0	0.0	0.0
F6 (Bohachevsky Nr.3)	2	0.0	0.0	0.0	0.0
F7 (Branin)	2	0.398891	0.397887	0.398055	0.397887
F8 (De Jong)	3	0.0	0.0	0.0	0.0
F9 (Easom)	2	-0.999725	-1.0	-0.98863	-1.0
F10 (Goldstein Price)	2	3.00006	3.0	3.00002	3.0
F11 (Hartman with $n = 3$ )	3	-3.86271	-3.86278	-3.86277	-3.86278
F12 (Hartman with $n = 6$ )	6	-1.84847	-3.32237	-3.32192	-3.32237
F13 (Hump)	2	8.86897e-05	4.65327e-08	0.000439177	0.0
F14 (Hyper-Ellipsoid)	30	1697.83	4.20078e-06	1.76103	0.0
	5	0.0257144	1.02076e-10	0.0120519	0.0
	10	0.0129742	9.06744e-10	0.0317808	0.0
	20	2.34247e-06	5.48692e-09	0.0136671	0.0
	30	0.00193177	2.12137e-08	0.785024	0.0
F15 (Levy Nr.2)	50	0.616365	6.12211e-08	2.07428	0.0
	5	0.0218405	3.8796e-09	0.000743298	0.0
	10	0.00617594	1.35077e-08	0.000173664	0.0
	20	0.0	1.28154e-07	0.00358961	0.0
	30	0.000140932	4.54418e-07	0.000992482	0.0
F16 (Levy Nr.3)	50	1.20497	1.68793e-06	1.32839e+06	1.60169e-06
	2	-1.95063	-1.8013	-1.95217	-1.8013
	4	0.00245258	0.000487242	0.0766711	0.000174267
	10	-21.0244	-209.998	-203.925	-209.999
	2	0.0	2.36476e-10	0.0	0.0
F20 (Rastringins Nr.1)	3	0.0	3.91857e-10	0.995047	0.0
	5	0.0	3.25394e-08	5.97189	0.0
	7	0.0	1.93565e-07	8.95636	0.0
	10	1.99124	1.98263e-06	32.8386	1.98263e-06

Table 2: The Optimal objective function values of SAES( $\mu + \lambda$ )Algorithm and SA-SAES( $\mu + \lambda$ ) Algorithm, and SACEP Algorithm and SA-SACEP Algorithm (continuation)

Function	# of variables	SAES( $\mu + \lambda$ )	SA-SAES( $\mu + \lambda$ )	SACEP	SA-SACEP
F21 (Rosenbrock)	2	0.0079492	5.68257e-07	0.00856004	2.096e-06
	5	0.915901	0.000190216	0.00588099	3.13482e-05
	10	4.104	3.83856e-05	2.15272	0.000239605
F22 (Schaffer Nr.1)	2	0.0	0.0	0.0	0.0
F23 (Schaffer Nr.2)	2	0.0	0.195296	0.0	0.195296
F24 (Shekel-5)	4	-5.04985	-5.27766e+13	-5.05082	-5.27766e+13
F25 (Shekel-7)	4	-5.0606	-5.27766e+13	-5.05484	-5.27766e+13
F26 (Shekel-10)	4	-5.1273	-5.27766e+13	-5.11435	-5.27766e+13
F27 (Shubert Nr.1)	2	-186.731	-186.731	-186.731	-186.731
F28 (Shubert Nr.2)	2	-186.341	-186.731	-186.731	-186.731
F29 (Step)	5	-144.0	0.0	-2848	0.0
	10	-366	0.0	-1.18937e+07	0.0
	50	-13864	0.0	-7.19852e+34	0.0
F31 (Zimmermanns)	2	-103.806	-494.741	-494.748	-494.735
F32 (Neumaier, 2010)	2	0.0	4.19095e-06	0.0	4.19095e-06
	5	0.0	6.11739e-05	0.0	6.11739e-05
	10	0.0	0.000461433	0.00287121	0.000553783
	50	0.681216	6.26669e-13	15.1833	0.017286
F33 (Neumaier, 2010)	2	0.0	6.26669e-13	0.0	0.0
	5	0.0	4.16862e-06	0.0	4.16862e-06
	10	8.06556	0.0113471	0.0	0.0322543
	50	11206.3	1030.77	6733.64	894.608
F34 (Neumaier, 2010)	2	0.0	1.78348e-05	0.0	1.78348e-05
	5	0.0	0.000742218	0.0	0.000742218
	10	0.0	0.00371919	0.0	0.00371919
	50	79.0741	0.189135	14.1295	0.189135
F35 (Neumaier, 2010)	2	0.0	0.0	0.0	0.0
	5	0.0	0.0	0.0	0.0
	10	0.0	0.0	0.0	0.0
	50	52.0	0.0	33.0	0.0
F36 (Neumaier, 2010)	2	5.03179e-06	8.18303e-07	4.59426e-06	8.18303e-07
	5	2.03186e-05	1.28561e-05	0.000226618	6.52515e-06
	10	0.000277681	6.09379e-05	0.001168	6.73284e-05
	50	415.836	0.00306063	380.029	0.00440367
F37 (Neumaier, 2010)	2	-837.931	-837.966	-3947.21	-837.966
	5	-1796.66	-2094.91	-1513.87	-2094.91
	10	-3809.75	-4189.83	-3245.56	-4189.83
	50	-18813.3	-20949.1	-12809.6	-20949.1
F38 (Neumaier, 2010)	2	0.0179898	6.08096e-11	0.00202397	0.0
	5	0.0744221	9.45082e-09	0.0409532	0.0
	10	0.0019571	1.13757e-07	0.0114677	0.0
	50	7.73384	4.46473e-05	10.5956	4.02717e-05
F41 (Neumaier, 2010)	2	-4.12397	-4.12398	-4.12373	-4.12398
F42 (Neumaier, 2010)	2	0.398891	0.397887	0.398055	0.397887
F43 (Neumaier, 2010)	2	3.00006	3.0	3.00002	3.0

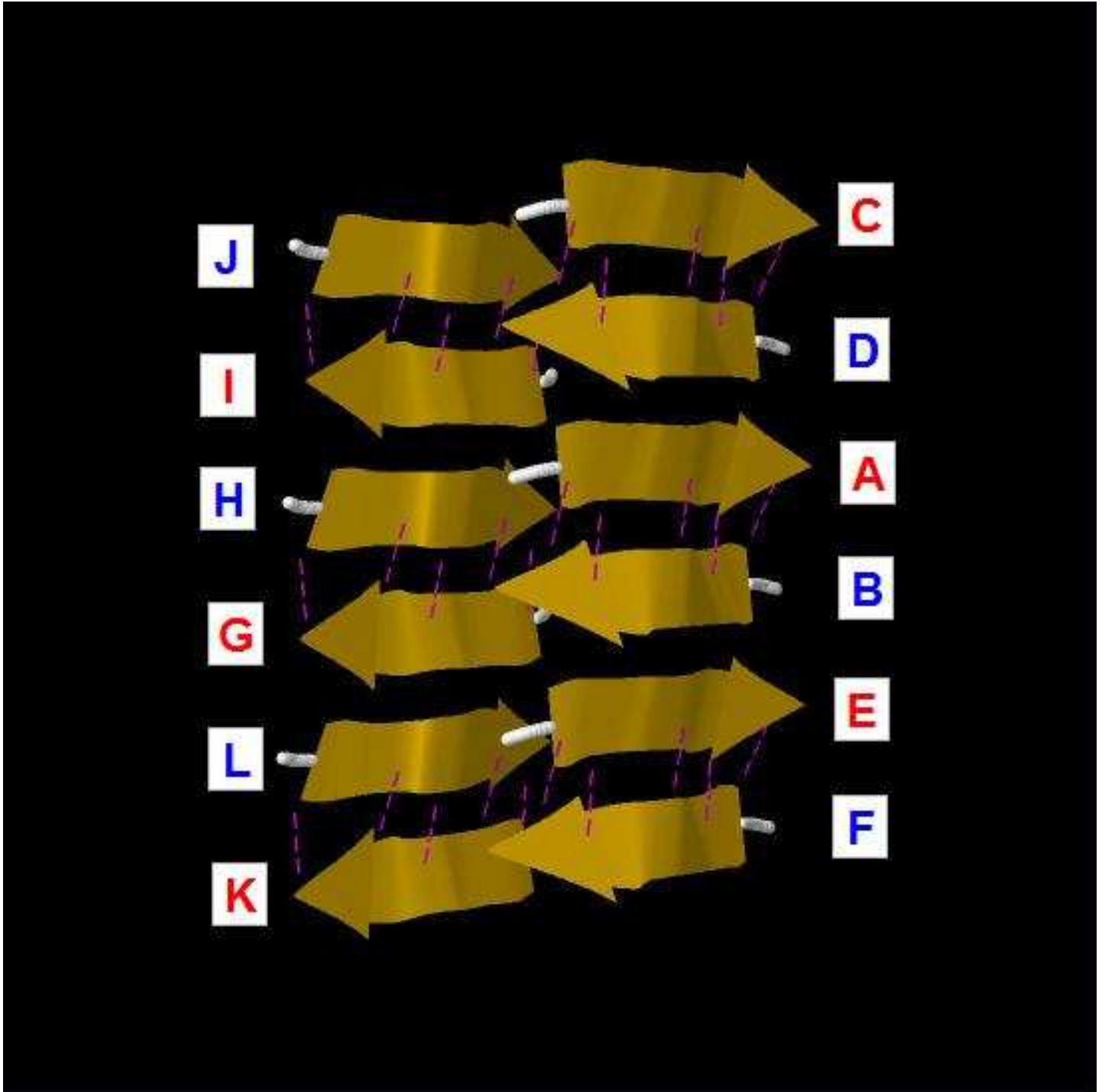
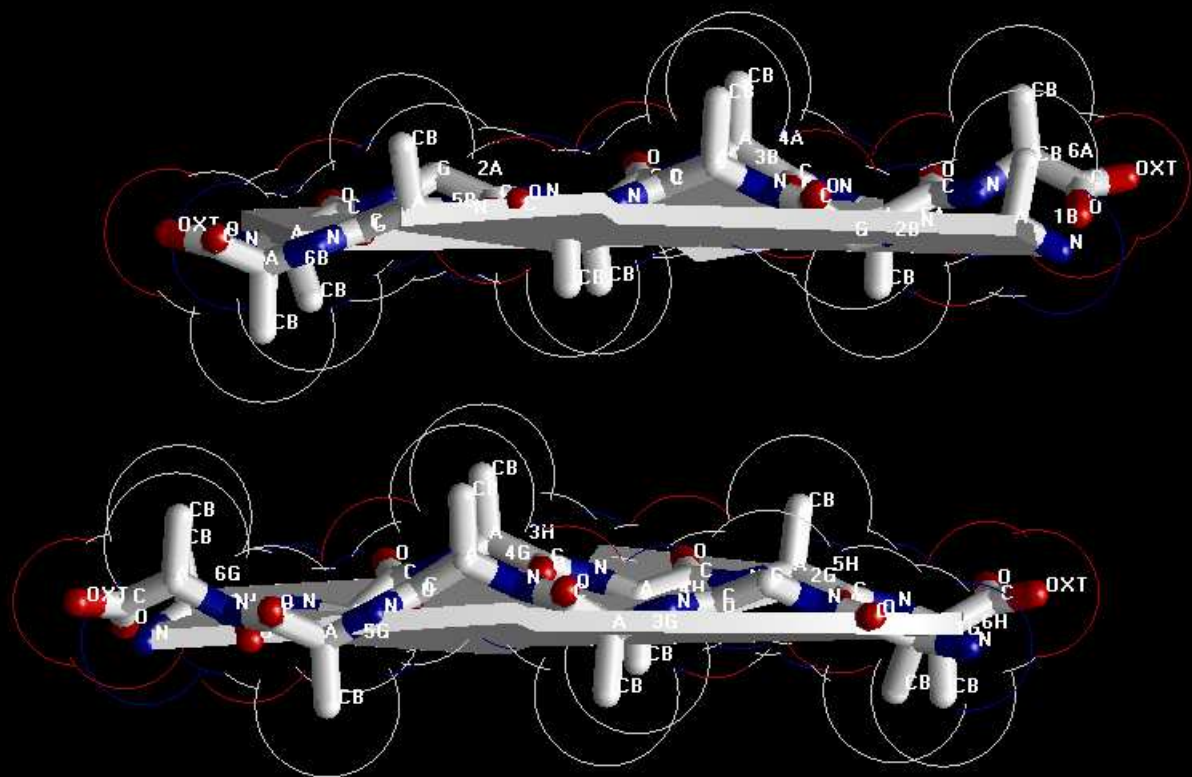
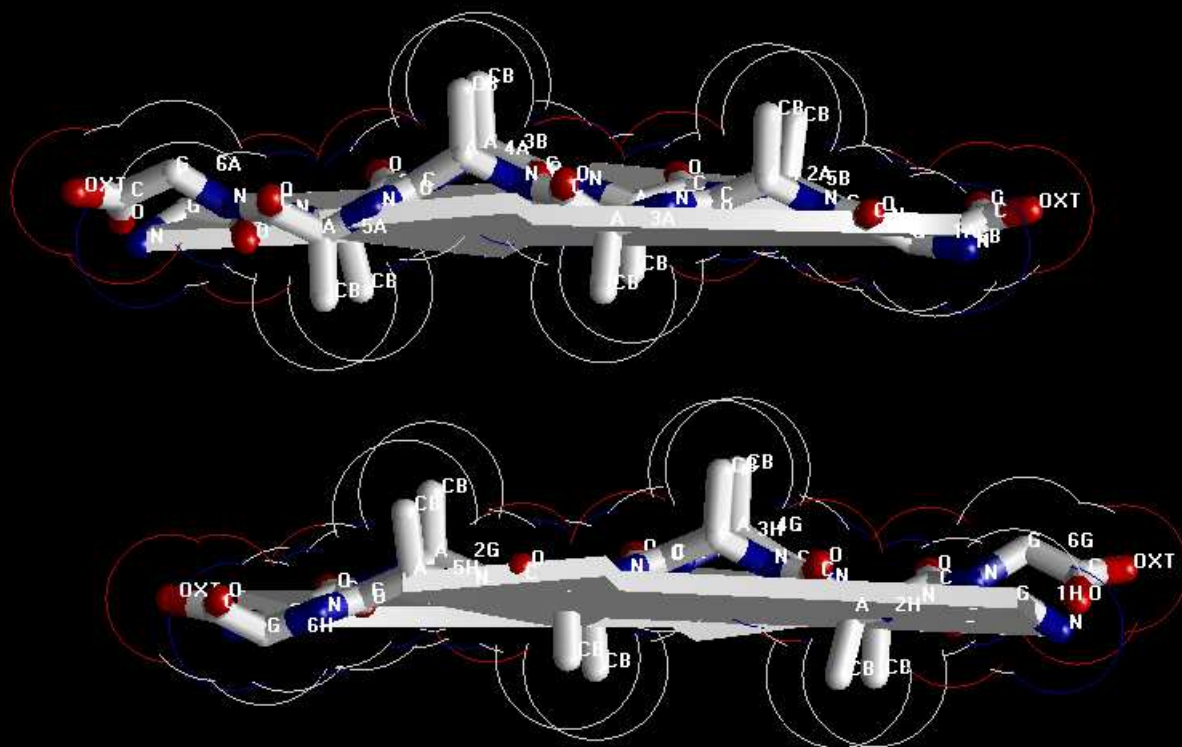


Figure 1: Protein fibril structure of human M129 prion GYMLGS (127–132). The purple dashed lines denote the hydrogen bonds. A, B, ..., K, L denote the 12 chains of the fibril.





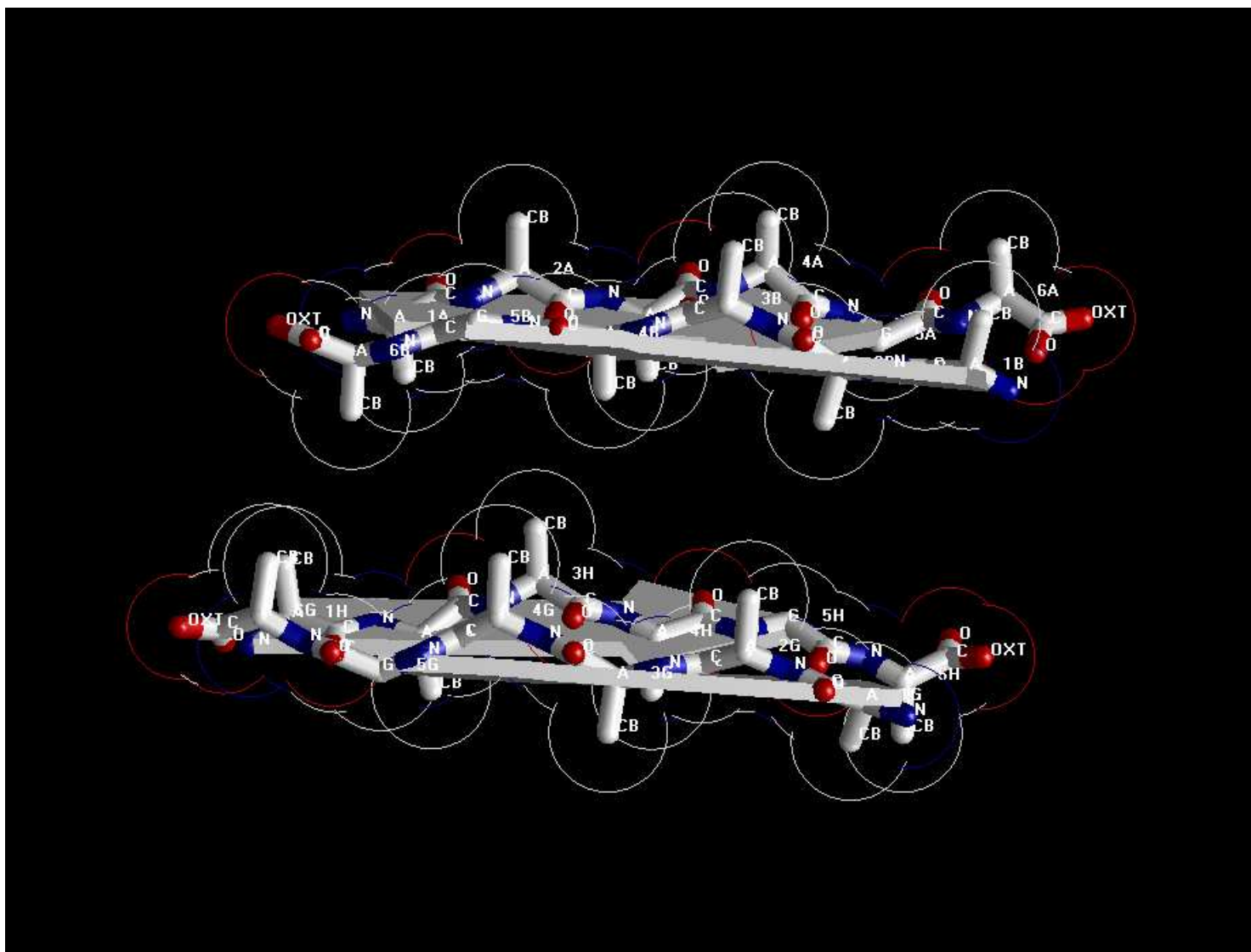
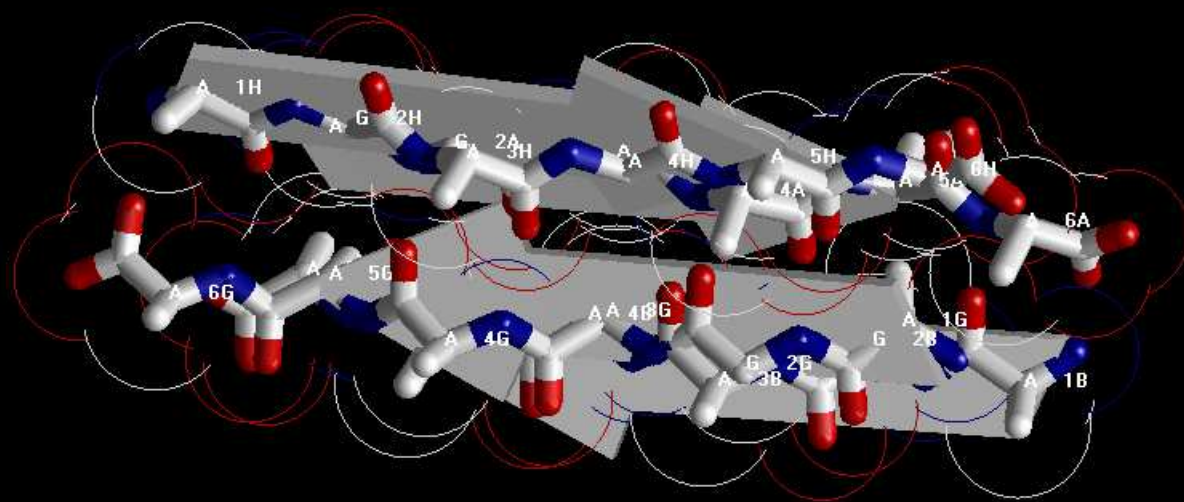
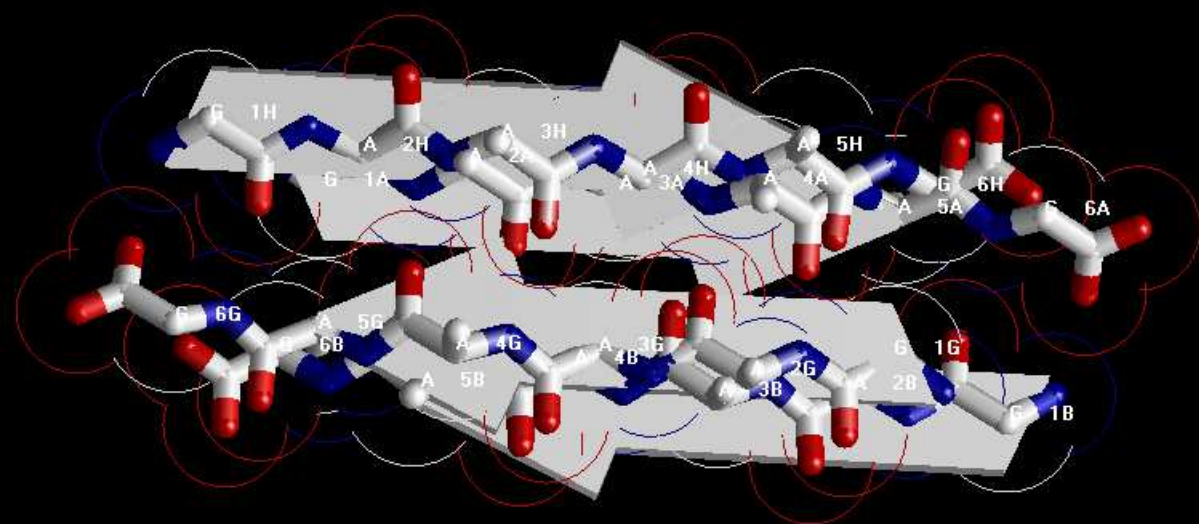


Figure 2: Far vdw contacts of AG chains and BH chains of Models 1-3.







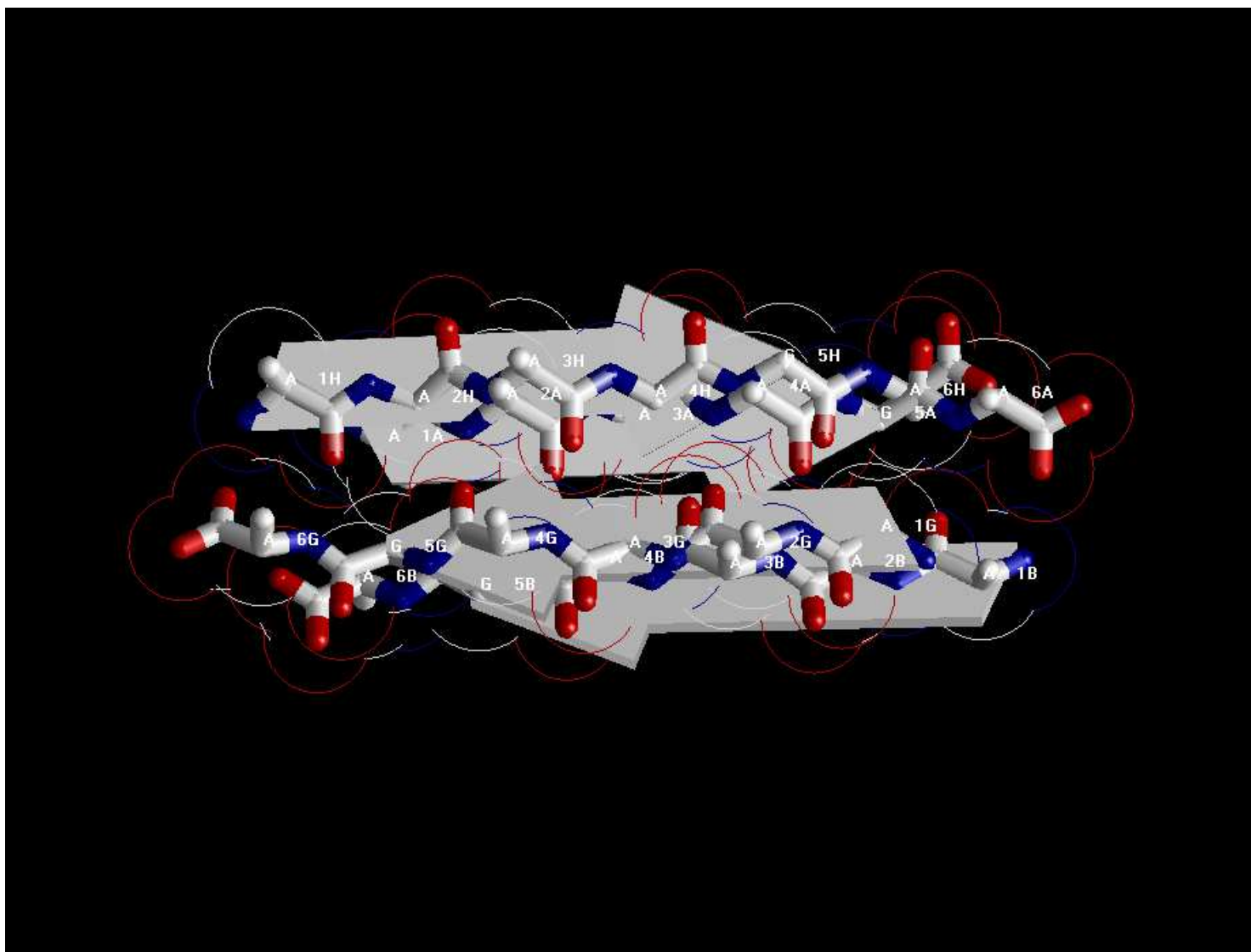
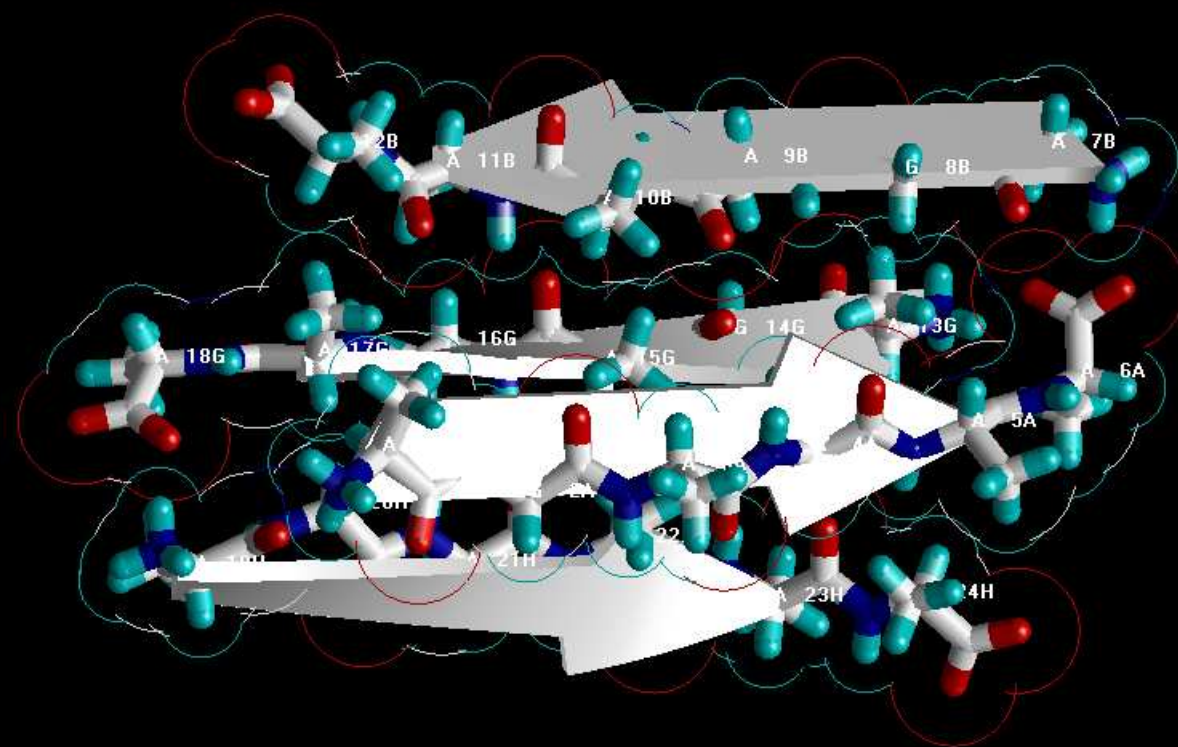
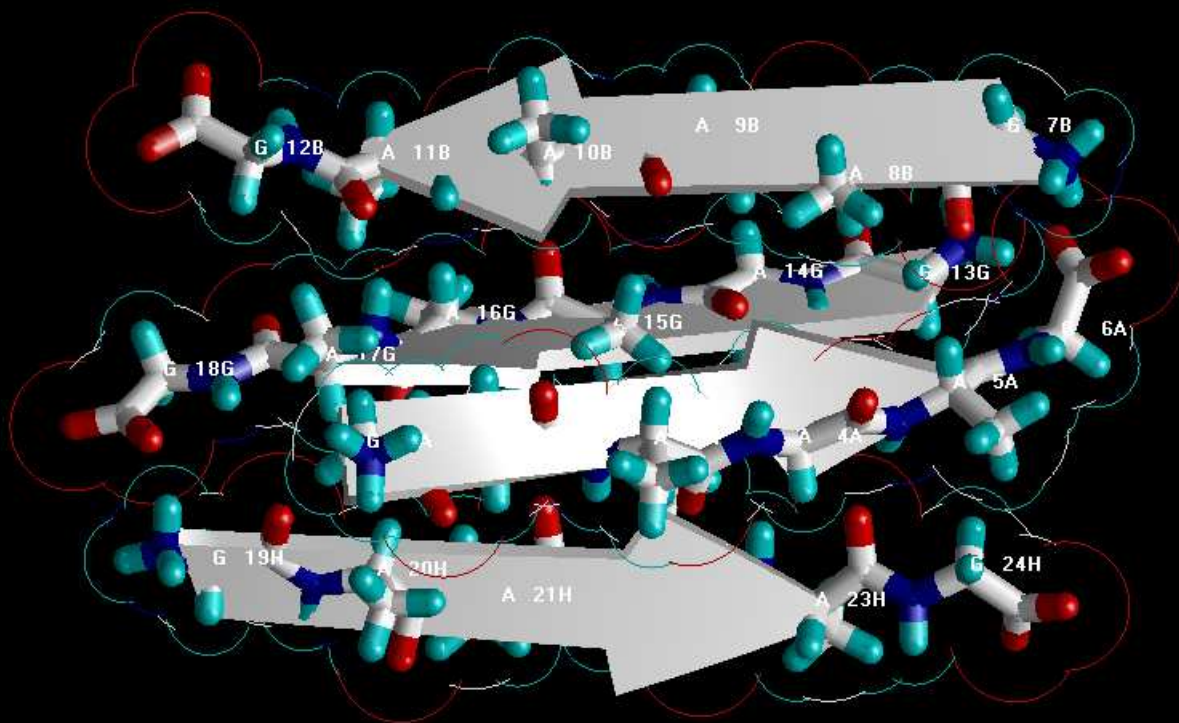


Figure 3: Close vdw contacts of AG chains and BH chains of Models 1-3.





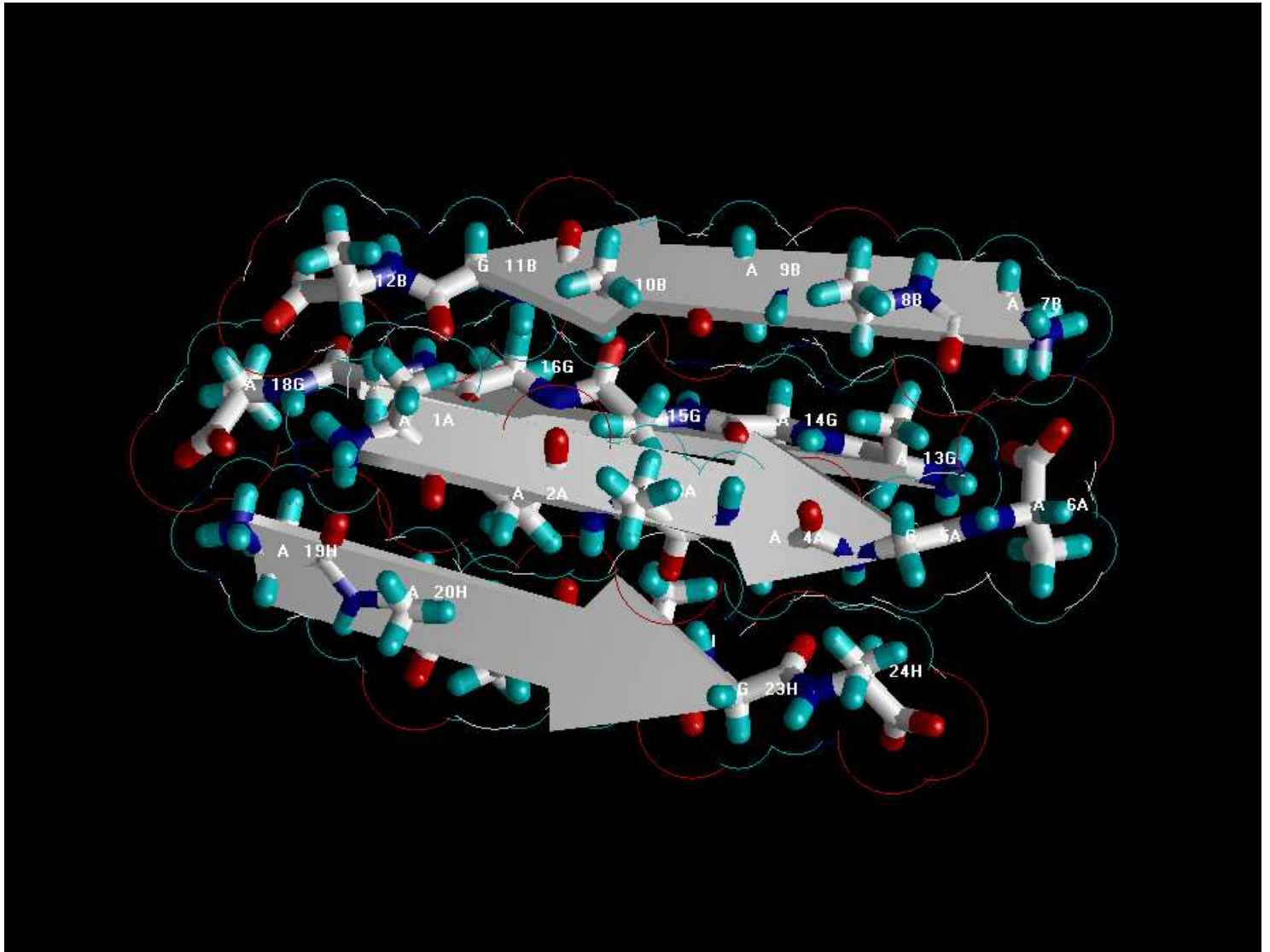


Figure 4: Optimal structures of prion AAAAGA amyloid fibril Models 1-3.